

# DELIVERABLE REPORT

**Grant Agreement number:** 688303

**Project acronym:** LUCA

**Project title:** Laser and Ultrasound Co-Analyzer for thyroid nodules

**Funding Scheme:** H2020-ICT-28-2015

**Deliverable reported:** D4.3 Provision of an optical-ultrasound phantom kit

**Due date:** 31.07.2017

**Name, title and organisation of partner:**

Alberto Dalla Mora, WP4 Leader, Politecnico di Milano (POLIMI)

Partners: ICFO, IDIBAPS, HEMO, VERMON, ECM, UoB

**Project website address:** [www.luca-project.eu](http://www.luca-project.eu)



## Content

1) Objectives.....	3
2) Design of the phantom box.....	5
3) DCS validation .....	8
4) US validation .....	9
5) Conclusions .....	11





## 1) Objectives

The objective of Deliverable D4.3 is the provision of an optical-ultrasound phantom kit. The phantom kit should satisfy the needs of the three different techniques of the LUCA device, Time-Resolved Spectroscopy (TRS), Diffuse Correlation Spectroscopy (DCS) and Ultrasound (US). Furthermore, the phantom kit has to reproduce the schematic geometry of the thyroid region, consisting in different layers with different optical, dynamic and acoustic properties.

In this document, we present the phantom kit provided to the consortium with the purpose to validate the LUCA demonstrator in laboratory settings. Its main feature is the possibility to carry out combined measurements with the above-mentioned techniques.

The validation of the solutions employed for the proposed kit is already contained in previous LUCA deliverables, in particular:

- 1) In Deliverable D4.1, "*Designs of a dynamic phantom for TRS-DCS*", we have proposed the use of mixtures of water and glycerol to fabricate liquid phantoms featuring different scatterer Brownian diffusion coefficients. Indeed, the medium viscosity depends on the concentration of glycerol in water, thus affecting the dynamic properties of the scattering particles. However, since the refractive index of glycerol ( $\sim 1.473$ ) is close to that of the fat droplets ( $\sim 1.45$ ) in the commonly used fat emulsions for liquid phantoms (Lipofundin, Liposyn, Intralipid), the scattering power of the fat droplets depends on the glycerol concentration. Therefore, the concentration of fat emulsion must be tuned in order to obtain phantoms with same optical properties, but different dynamic properties.
- 2) Also, in D4.1, "*Designs of a dynamic phantom for TRS-DCS*", we have proposed the use of Mylar sheets to separate different liquid layers to fabricate multi-compartment phantoms. Mylar foils were already validated in the literature for TRS, therefore we have extended their validation also for DCS. Hence, we proved that Mylar sheets, under certain conditions (thickness, colour etc.), can be considered invisible to both TRS and DCS.
- 3) In Deliverable D4.2, "*Designs of phantom for TRS-DCS and ultrasound*", we have extended the validation of water-glycerol mixtures to US. To this purpose we have verified that both the speed of sound (SOS) and the attenuation of the US waves are in the order of magnitude of the human tissues. However, since there is a variation of few percent in the SOS depending on the glycerol concentration, there could be the need to take into account this variation in the analysis algorithm.
- 4) Also, in D4.2, "*Designs of phantom for TRS-DCS and ultrasound*", we have proved that Mylar sheets present a strong contrast to US, almost independently of the foil thickness. They can be therefore exploited not only to separate liquid compartments, but also to simulate US contrast due to different anatomical structure.

Thanks to these findings, we have decided to make use of a phantom box previously developed at the Physics Department of POLIMI for its activity towards the standardization of diffuse optics systems (design presented in Section 2). This box is a 2-layer system where the two compartments are separated by a thin Mylar sheet. Two different phantoms can therefore be used to fill the two compartments, thus allowing exploiting the first layer to simulate the superficial tissue above the thyroid (skin, adipose, muscles, etc.) and the bottom layer to simulate the thyroid tissue.

The box has been developed as an upgrade of a previously validated box for TRS systems. Its suitability to TRS measurements has already been demonstrated in previous works, e.g. [F. Martelli et al., "*Phantoms for diffuse optical imaging based on totally absorbing objects, part 2: experimental implementation*," *Journal of Biomedical Optics* 19(7), 076011, 2014]. Therefore, to prove the suitability



of the box for LUCA purposes, we carried out DCS and US measurements. Since the LUCA system is not yet developed, we combined state of the art systems operating in parallel on the phantom box.

This report is organized as follows: Section 1 highlights objectives, Section 2 reports the design of the core part of the phantom kit, Section 3 demonstrates the suitability of the phantom box to DCS, in Section 4 the US system was used to check the quality of US images taken inside the proposed box and, finally, conclusions are discussed in Section 5.

## 2) Design of the phantom box

The cell is made by three parts. In part A and B, a Mylar sheet of 50  $\mu\text{m}$  thickness is held by two PVC plates, designed as shown in Figure 1 to guarantee water tightness. Part A can be moved along the axis of the system so that the distance between the two Mylar windows can vary from 5 mm up to 20 mm. Part B and Part C are fixed so that the distance of the Part B windows to Part C is 60 mm. Part A and Part B and Part B and Part C are closed on the sides by two rubber layers held watertight by three metal bands, as shown in Figure 2.

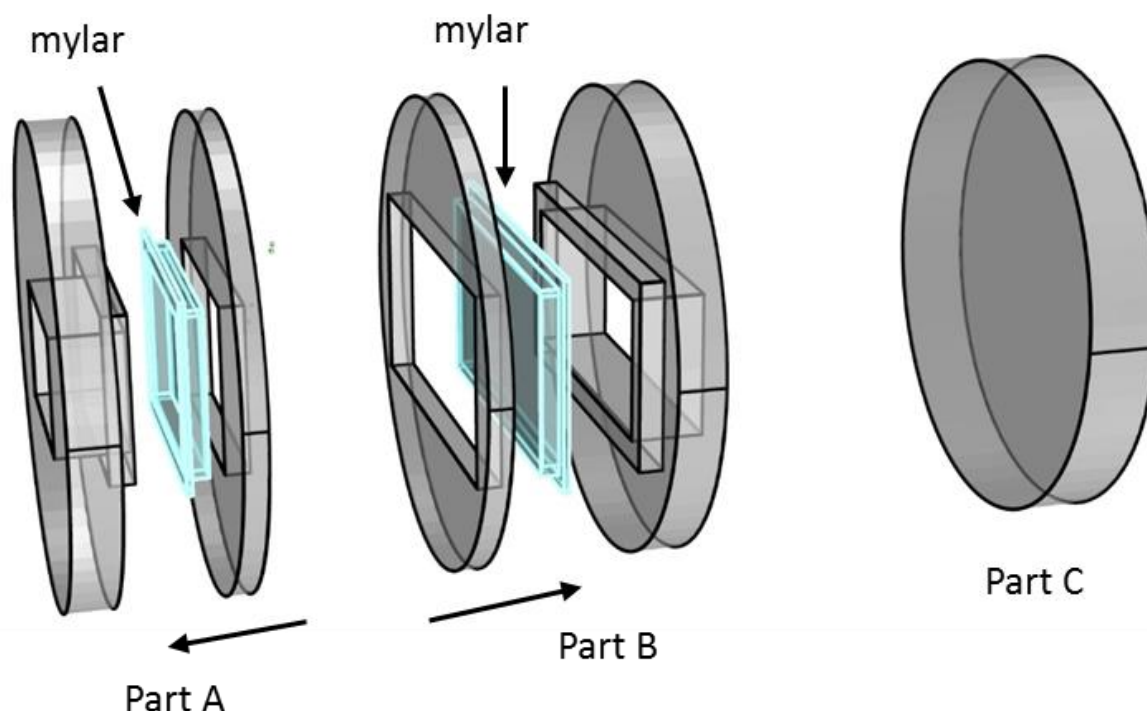


Figure 1 Schematic of the bilayer cell.

Figure 2 shows two photographs taken during a measurement campaign performed at ICFO in collaboration with POLIMI (see next Sections). In the top photograph it is possible to see a probe with optical fibres entering in the window of the Part A, touching the thin sheet of Mylar that allows probing the phantom with both optical and US investigations. The effectiveness of Mylar to enclose the phantom was demonstrated in Deliverable D4.2 “*Designs of phantom for TRS-DCS and ultrasound*”. In particular, it was demonstrated that a Mylar sheet can be used between the probe and the phantom without compromising the quality of US images. Additionally, in Deliverable D4.1 “*Designs of a dynamic phantom for TRS-DCS*”, it was demonstrated that Mylar sheets are invisible to optical techniques, as it is desirable to be sensitive only to the liquid phantom optical properties.

The thickness of the top layer (i.e. the distance between the Mylar sheet in Part A and the Mylar sheet in Part B) can be set just by rotating the knob visible on the right side of Figure 2 (bottom). The knob moves Part A along two rails, thus changing the distance between the Mylar sheets. This layer mimics the properties of the most superficial tissues like skin and muscle. The liquid phantom between Part B and Part C mimics the deeper layer (i.e. the thyroid tissue). In this case the thickness is fixed to 6 cm, which is well beyond the maximum depth that can be probed with optical techniques (i.e. 2-3 cm),

thus ensuring to have no effect from the presence of the Part C, which is used to enclose the phantom. The 2 layers are therefore separated by the Mylar sheet of Part B. Being invisible to optical techniques, but clearly visible to US investigations, as it was demonstrated in Deliverable D4.2 “*Designs of phantom for TRS-DCS and ultrasound*”, it allows to retrieve the top layer thickness from the US measurement, mimicking what happens during real in vivo measurements.

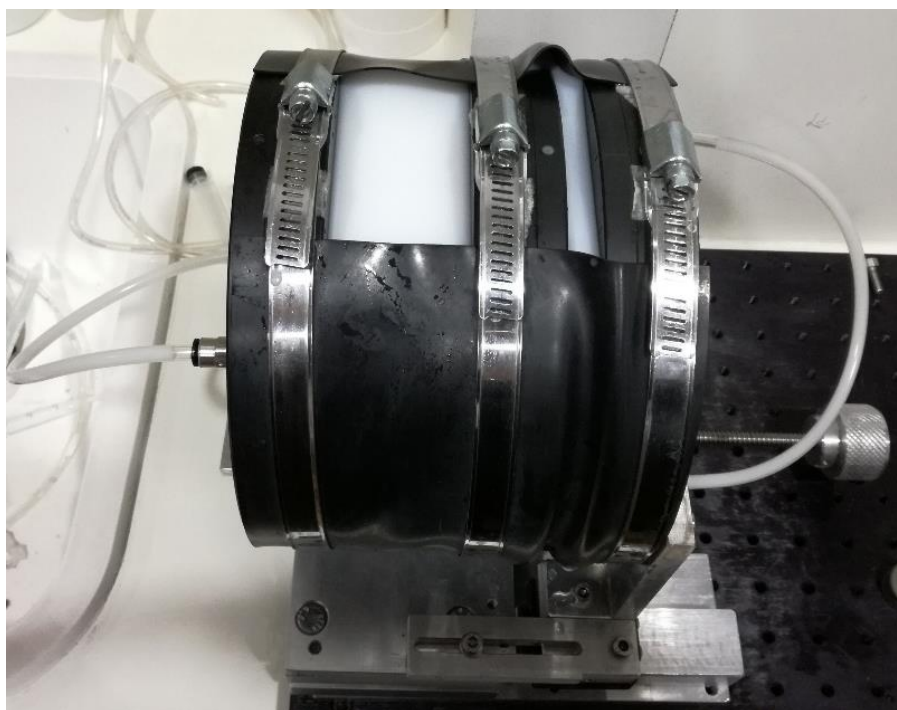
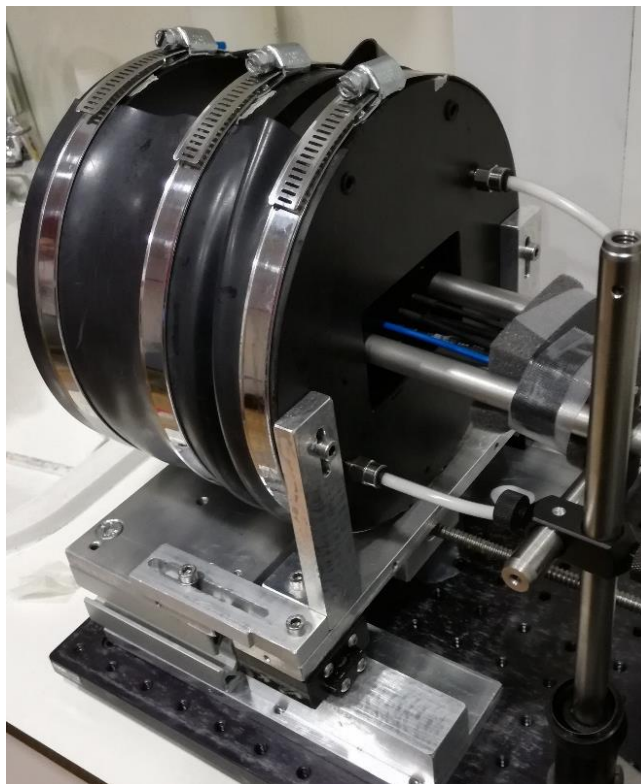


Figure 2 Photographs of the phantom box taken during the measurement campaign at ICFO.



Finally, each layer of the cell is connected to a pump through rubber pipes. The pump can be turned on by applying a 12 V bias supply, thus enabling an automatic stirring of the phantom by taking it at the bottom of the cell and putting it back in the upper part of the cell. This stirring system is particularly useful for measurements for which there is the need to continuously add ink, Lipofundin and/or glycerol to the phantom, with the need to reach each time a homogeneous dispersion.

### 3) DCS validation

In this section we report the tests performed in order to validate the layered phantom box for DCS measurements. To this purpose, we have measured liquid phantoms consisting of solution of water and glycerol with Lipofundin20% as the scattering element (see Deliverable D4.1 and D4.2). We have considered four homogeneous phantoms with four different concentrations of glycerol (0%, 10%, 20%, 30%) with a fixed reduced scattering coefficient  $\mu_s' = 5 \text{ cm}^{-1}$  (Lipofundin concentrations according to recipe reported in Deliverable D4.2) and the same absorption coefficient of water. For each of these four phantoms, we have performed DCS measurements at 785 nm wavelength using both a non-layered phantom box and the LUCA layered phantom box described in the previous section (both layers filled with the same liquid). These tests aim to determine if the new layered phantom box introduces sensible changes and artefacts in the DCS signal.

The results are reported schematically in Figure 3a and Figure 3b. In Figure 3a, we report the measured scatterer Brownian diffusion coefficients,  $D_b$ , for the phantoms both in the non-layered reference box and in the LUCA layered phantom box, for two different source detector separations (long SDS 2.44 cm, short SDS 1.44 cm).

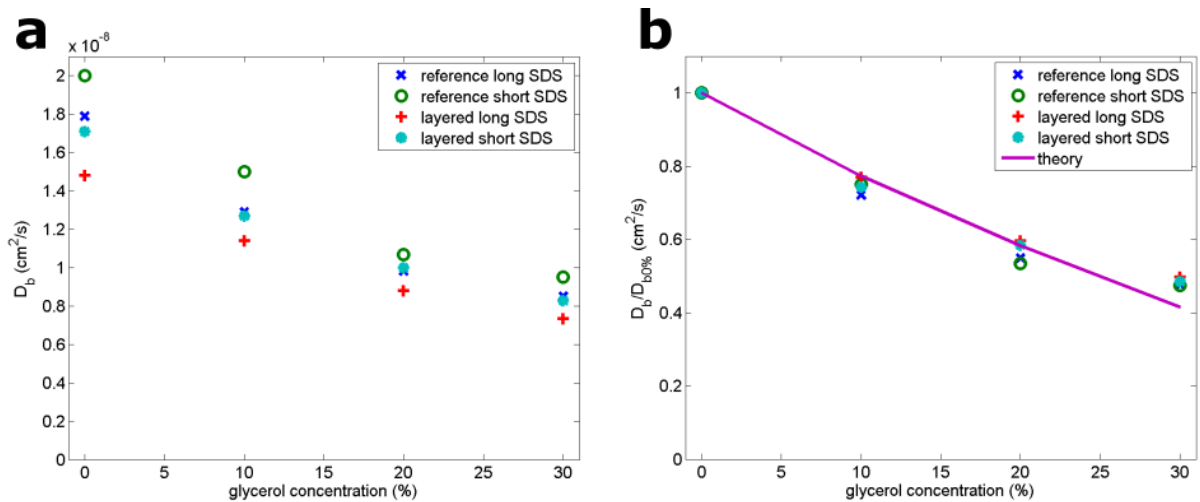


Figure 3 a)  $D_b$  measured using both the reference non-layered phantom box and the LUCA layered phantom box, for 4 phantoms with different glycerol concentrations and 2 different source-detector separations (SDS). b) Ratio of the measured  $D_b$  ( $D_b/D_{b0\%}$ ) compared to the prediction of the theory.

The measured  $D_b$  for each glycerol concentration results in good agreement with the theoretical prediction. The small differences can be due to possible imprecision in measuring the source-detector separations, and also in changes in environmental conditions (e.g. temperature) between the measurements with the reference box and the layered box.

In Figure 3b, we report the ratio between the measured  $D_b$  for varying glycerol concentration and  $D_b$  with no glycerol in the liquid solution ( $D_b/D_{b0\%}$ ). These ratios are compared with the prediction of the theory, which states that the ratio between the Brownian diffusion coefficients are inversely proportional to the ratio of the viscosities,  $\eta$ , of the two liquids ( $\frac{D_{b1}}{D_{b2}} = \frac{\eta_2}{\eta_1}$ ). Figure 3b shows clearly that the results of all the measurements agree with what was expected from the theory.

The results reported demonstrate that the geometry and the components of the new LUCA layered phantom box do not alter the DCS signal. Although it was expected since the measurements reported in Deliverable D4.1 showed that the material used to separate different layers (Mylar thin pellicles) does not alter DCS curves, these results represent a first validation of the LUCA phantom box for DCS.

#### 4) US validation

In this section we report the ultrasound measurements performed to validate the layered phantom box. They have been acquired using a standard LC1038V probe (embedding the same acoustic transducer as the LUCA probe) combined with the ECM Exapad ultrasound system. The experiment consisted in taking ultrasound images of the phantom box filled with solutions of water and glycerol at different concentrations (for these experiments we did not add to the solutions Lipofundin, which is an optical scattering element and does not affect acoustic waves). The bottom compartment of the phantom box has been filled with only water while the top layer of the phantom with four different solutions of water and glycerol. The thickness of the top layer has been set at 10 mm. We acquired US images keeping fixed the liquid in the bottom layer, and considering for the top layer solutions of water and glycerol with glycerol concentrations of 0%, 10%, 20% and 30%. The ultrasound probe has been placed, as done for the optical probe (see Figure 2 top), in contact with the frontal Mylar window. The transmission of the acoustic waves was guaranteed by using the proper ultrasound gel in front of the probe transducer.

Figure 4 shows an example of acquisition, highlighting the effects already discussed in the Deliverable D4.2, “*Designs of phantom for TRS-DCS and ultrasound*”. In this case the phantom box was filled with pure water in both layers. On top of the image, close to the phantom surface, it is possible to see the typical ringdown due to multiple trips of the US wave inside the first Mylar sheet, which is used to enclose the phantom. At a depth of about 1 cm, as expected, the image shows the echo from the inner sheet of Mylar, which is used to separate the two compartments, again with the associated ringdown. More in depth, as discussed in Deliverable D4.2, there are artefacts due to multiple reflections of the US wave between the two Mylar sheets.

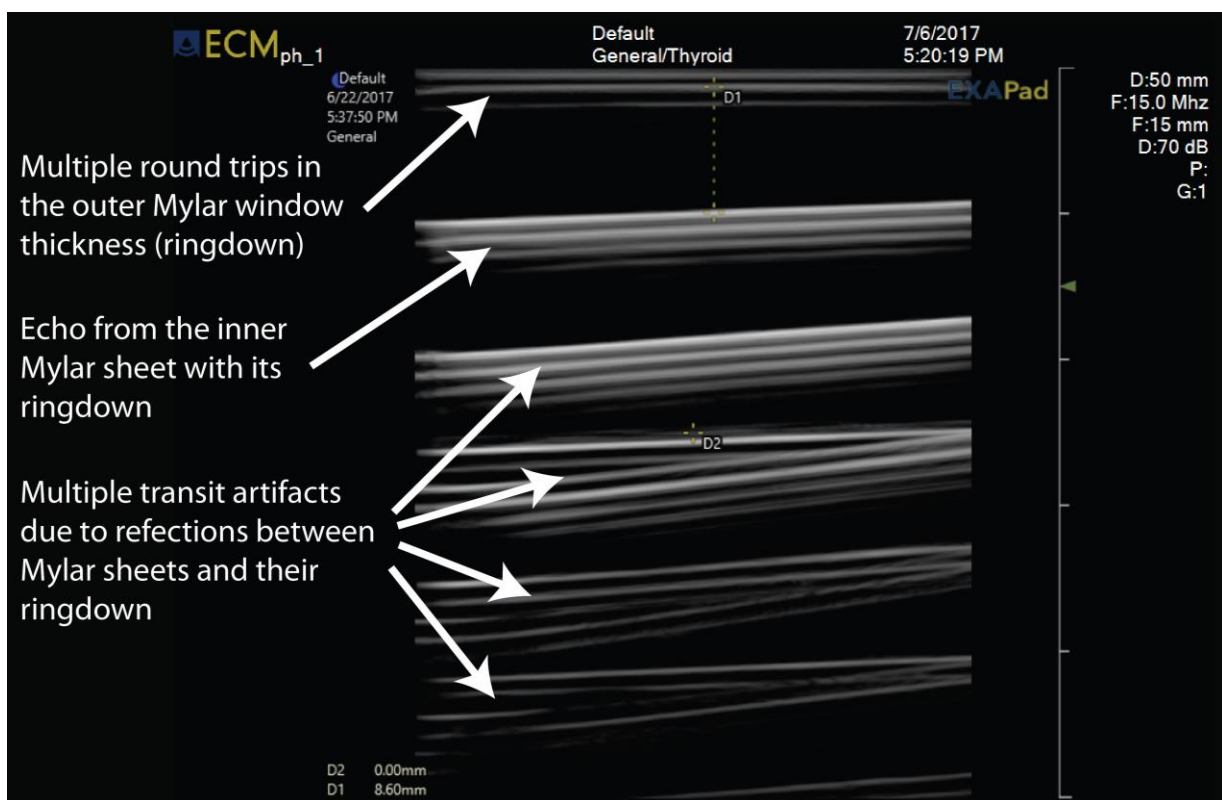


Figure 4 Example of ultrasound image, acquired with pure water in both the top and the bottom layers.

The images acquired with different glycerol concentrations in the top layer are reported in Figure 5. Notwithstanding the multiple echoes and ringdown, from the ultrasound images acquired we are able to measure the depth of the bottom layer, as shown in the Figure 5 with the dotted vertical line (D1) connecting the two markers. We measured 8.60 mm, 8.77 mm, 8.7 mm and 8.68 mm respectively for the top layers of 0% glycerol, 10% glycerol, 20% glycerol and 30% glycerol concentration. The depths measured slightly differ from what manually set rotating the knob of the phantom (10 mm). This difference can be ascribed to the pressure made by the ultrasound probe on the front Mylar window, applied to have a good contact and to obtain images with better quality, as it will happen during measurements performed in vivo. This effect makes almost negligible the small dependence of the SOS with the glycerol concentration, which can produce an error of just  $\sim\pm 0.5$  mm if not corrected by setting proper reference SOS in the US machine.

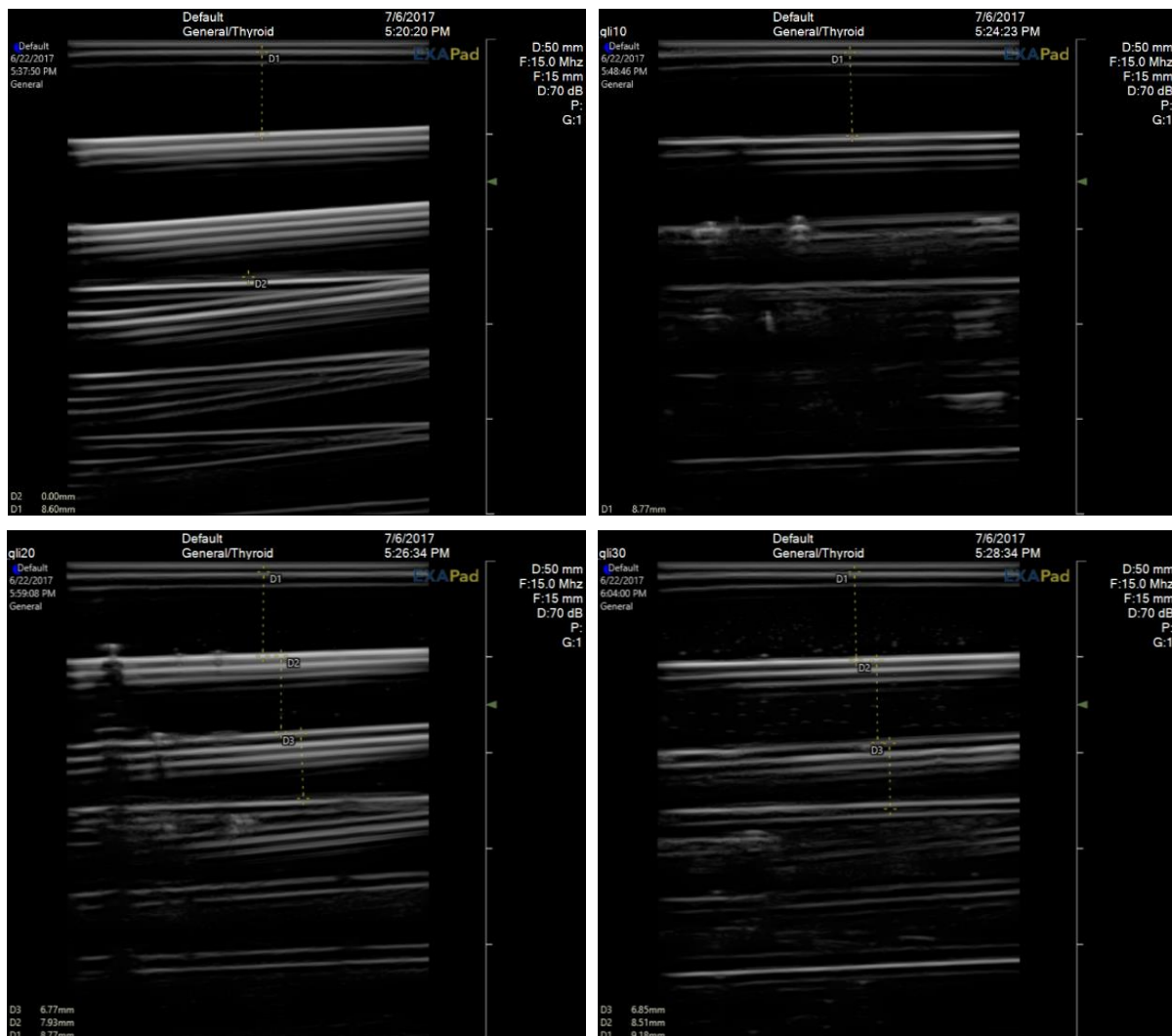


Figure 5 Ultrasound images acquired for a fixed content of the bottom layer (pure water) and 4 different water/glycerol solutions in the top layer. Top left: glycerol 0%. Top right: glycerol 10%. Bottom left: glycerol 20%. Bottom right: glycerol 30%.



## 5) Conclusions

In conclusion, we provided an optical-ultrasound phantom kit consisting in a bilayer phantom box. The liquid phantom can be fabricated following the recipe based on water/glycerol solutions plus Lipofundin presented in Deliverables D4.1 and D4.2, thus obtaining well-known and tunable optical and dynamic properties. The box consists in a structure allowing the use of bilayer phantoms, with compartments separated by a thin Mylar window, which is invisible, as desired, to both TRS and DCS. The access of the optical-ultrasound probe from outside of the box is guaranteed by an additional frontal Mylar window. The top layer has a tunable thickness (that can be changed rotating a knob), while the bottom layer has a fixed thickness of 6 cm. An automatic stirring system is also provided, thus simplifying the execution of linearity tests, when optical/dynamic properties must be linearly changed by adding glycerol/Lipofundin/ink to the original solution. The described phantom kit has already been validated for TRS in previous studies. Here we have demonstrated the suitability to DCS (results in section 3) and for ultrasound investigations (results in section 4).